Heat treatment alleviates the growth and photosynthetic impairment of transplastomic plants expressing *Leishmania infantum* Hsp 83-*Toxoplasma gondii* SAG1 fusion protein

Mariana G. Corigliano[1*], Romina M. Albarracín[1*], Juan M. Vilas[2], Edwin F. Sánchez López[1], Sofía A. Bengoa Luoni[1], Bin Deng[3], Inmaculada Farran[4], Jon Veramendi[4], Santiago J. Maiale[2], Valeria A. Sander[1], and Marina Clemente[1+]

[1]Laboratorio de Biotecnología Vegetal, IIB-INTECH, CONICET-UNSAM, Chascomús, Provincia de Buenos Aires, Argentina.

[2]Laboratorio de Estrés Abiótico en Plantas, IIB-INTECH, CONICET-UNSAM, Chascomús, Provincia de Buenos Aires, Argentina.

[3]Marsh Life Science Building, Rm 337. University of Vermont Burlington, Vermont, United States of America.

[4]Instituto de Agrobiotecnología, Universidad Pública de Navarra-CSIC, Campus de Arrosadía, Pamplona, Spain.

* Mariana G. Corigliano and Romina M. Albarracín have contributed equally to the work.

[+] Corresponding authors.

E-mail addresses: mclemente@intech.gov.ar (M. Clemente)

ABSTRACT

Previously, we showed that transplastomic tobacco plants expressing the LiHsp83-SAG1 fusion protein displayed a chlorotic phenotype and growth retardation, while plants expressing the SAG1 and GRA4 antigens alone did not. We conducted a comprehensive examination of the metabolic and photosynthetic parameters that could be affecting the normal growth of LiHsp83-SAG1 plants in order to understand the origin of these pleiotropic effects. These plants presented all photosynthetic pigments and parameters related to PSII efficiency significantly diminished. However, the expression of *CHLI*, *RSSU* and *LHCa/b* genes did not show significant differences between LiHsp83-SAG1 and control plants. Total protein, starch, and soluble sugar contents were also greatly reduced in LiHsp83-SAG1 plants. Since Hsp90s are constitutively expressed at much higher concentrations at high temperatures, we tested if the fitness of LiHsp83-SAG1 over-expressing LiHsp83 would improve after heat treatment. LiHsp83-SAG1 plants showed an important alleviation of their phenotype and an evident recovery of the PSII function. As far as we know, this is the first report where it is demonstrated that a transplastomic line performs much better at higher temperatures. Finally, we detected that LiHsp83-SAG1 protein could be binding to key photosynthesis-related proteins at 37 °C. Our results suggest that the excess of this molecular chaperone could benefit the plant in a possible heat shock and prevent the expected denaturation of proteins. However, the LiHsp83-SAG1 protein content was weakly decreased in heat-treated plants. Therefore, we cannot rule out that the alleviation observed at 37 ºC may be partially due to a reduction of the levels of the recombinant protein.

Keywords: Pleiotropic Effects, Transplastomic Plants, heat shock protein, Tobacco, *Toxoplasma gondii*

1. Introduction

In recent years, great efforts have been conducted to improve the yields of recombinant proteins produced in plants [1–3]. In this sense, chloroplast transformation has emerged as an alternative platform to raise the low yields obtained in transgenic plants [4,5]. The plastid transformation has allowed the increase of protein expression levels with respect to nuclear transformation since it is possible to find a large number of chloroplasts within a single leaf cell and, therefore, multiple copies of the transgene [5,6]. In addition, in contrast to nuclear transformation, in chloroplast transformation there are no positioning effect on the transgene because the transgene insertion into plastid DNA occurs via homologous recombination. Therefore, it is not necessary to evaluate several transformation events due to the genetic background in all transplastomic lines produced are identical [7]. Up to now, different kind of interesting proteins was expressed in transplastomic plants. Some of them are related to agronomic resources, phytoremediation and biofuels, while others correspond to pharmaceutical molecules and vaccine antigens [4]. It has been reported that some transplastomic lines present pleiotropic effects related to plant physiology, like plant growth retardation, chlorosis, and male sterility [8,9]. Some authors attributed these side effects to the transgene overexpression [10]. However, there are some examples where the pleiotropic effects are due to the presence of the recombinant protein since they disturb the chloroplast metabolism affecting the photosynthetic mechanism and, in consequence, the correct plant development [10].

Previously, the correct insertion and homoplasmy of *Toxoplasma gondii* GRA4, SAG1, and LiHsp83-SAG1 antigens were demonstrated [11,12]. In particular, SAG1 yields were significantly increased when this antigen was fused to the carrier/adjuvant *Leishmania infantum* Hsp83 (up to 100 μg/g of fresh leaves). Noticeably, all the leaves

from the LiHsp83-SAG1 transplastomic line showed a chlorotic phenotype and growth retardation [12]. Nevertheless, the expression levels reached for the LiHsp83-SAG1 line were not superior to 3% of the total soluble protein and it remained to be determined if the overexpression of LiHsp83-SAG1 would explain by itself the pleiotropic effects observed. Therefore, we conducted a comprehensive examination of the metabolic and photosynthetic parameters that could be affecting the normal growth of LiHsp83-SAG1 plants in order to understand the origin of these pleiotropic effects and whether there is a way to overcome them. The implications of such findings are discussed.

2. Materials and methods

2.1. Plant material and heat treatment

Transplastomic tobacco genotypes expressing SAG1, GRA4, and LiHsp83-SAG1 were generated as described in Del Yácono et al. [11] and in Albarracín et al. [12] and compared to wild-type non-transformed (WT) tobacco control (*Nicotiana tabacum* L. cv Petite havana). Since the insertion of transgenes into the plastid DNA occurs via homologous recombination at the specific *trnI-trnA* insertion site, all transplastomic lines are identical [7]. Therefore, the SAG1 line 1, the GRA4 line 1 and the LiHsp83-SAG1 line 1 were used in further experiments. Sterile seeds from transplastomic lines or WT plants were germinated in sterile Murashige Skoog medium (MS, Sigma) supplemented with sucrose 3% and agar 8 g/L) in a growth chamber with a 16 h day/ 8 h night photoperiod (photosynthetic flux photon density (PPFD) of 350 µmol quanta m^{-2} s^{-1}) provided by cool-white fluorescent lamps, 24 ± 2 °C temperature. After 21 days, ten plants per genotype were grown in sterile sand: soil: perlite (1:1:1) mixture and watered with Hoagland nutrient mix [13] every 2 days. Physiological, biochemical and gene expression analyses were performed between 20 and 40 days after transplantation (dat).

The heat treatment was administered at 37 °C for 3 weeks to 40-days-old WT and LiHsp83-SAG1 plants. Control plants were maintained at 25 °C the same period. At the end of the treatment, photosynthetic parameters were measured, and plants were immediately harvested and stored at -80 °C until their use for RNA isolation.

2.2. Foliar area

The youngest fully completely developed leaf was photographed, the images were analyzed with *Gel-Pro analyzer* software (Media Cybernetics) and the foliar area was calculated.

2.3. Estimation of chlorophyll content

Total chlorophylls of the youngest fully completely developed leaf were determined used an optical leaf-clip chlorophyllmeter (Cavadevices http://www.cavadevices.com, Argentina). Chlorophyll *a*, chlorophyll *b* and carotenoids were measured according to Lichtenthaler [14]. Briefly, 40 mg of plant material of every line and WT plants were ground in liquid nitrogen and incubated in 80% acetone with agitation in darkness overnight at 4 °C. The extracts were centrifuged at 5000 x g at 4 °C and the supernatant was saved. The absorbance was read at 470 nm, 663 nm and 647 nm in a spectrophotometer (Perkin Elmer Lambda 25 UV/VIS spectrometer), and pigments concentration was calculated according to Lichtenthaler [14], using the following formulas:

Chlorophyll “a” = 11,25 x $A_{\lambda 663}$ - 2,79 x $A_{\lambda 647}$

Chlorophyll “b” = 21,5 x $A_{\lambda 647}$ - 5,1 x $A_{\lambda 663}$

Carotenoids = (1000 x $A_{\lambda 470}$ - (1,82 x [Chl “a”] - 85,02 x [Chl “b”])/198) x 13,33

127 *2.4. Chlorophyll fluorescence fast-transient analysis*

128 The non-invasive OJIP analysis [15] was performed in the youngest fully
129 developed leaf with a portable chlorophyll fluorometer (Pocket PEA v.1.1, Hansatech
130 Instruments Ltd.). Leaves were pre-darkened 20 min before analysis. After that, they were
131 exposed during 3 s to 3500 μmol photons m^{-2} s^{-1} (637 nm peak wavelength) and
132 Chlorophyll *a* fluorescence was recorded. The data were analyzed with PEA Plus
133 software (Hansatech Instruments Ltd.). The maximum quantum yield of primary
134 photochemistry (Fv/Fm) was determined. In addition, the contribution to photosynthesis
135 regulation by the three functional steps namely ABS (absorption of light energy), TR
136 (trapping of excitation energy) and ET (conversion of excitation energy to electron
137 transport) was analyzed. The definition of each parameter is provided in Supplementary
138 Table 1.

139

140 *2.5. Gas Exchange determination*

141 The net photosynthesis (Pn), stomatal conductance (g_s) and CO_2 concentration of
142 sub-stomatal cavity (C_i) were measured in the youngest completely developed leaf at light
143 saturation (1500 μmol photons m^{-2} s^{-1} illumination led light) using an infrared gas
144 analyzer TPS-2 Portable Photosynthesis System (PP Systems In.).

145

146 *2.6. Protein extraction and quantitation*

147 For total protein extraction, the youngest completely developed leaf from
148 transplastomic lines and WT tobacco plants were ground in liquid nitrogen and
149 homogenized in Laemmli buffer (0.5 M Tris-HCl pH 6.5, 4% SDS, 20% glycerol, 10%
150 β-mercaptoethanol and 0.1% bromophenol blue) in a 1:3 ratio. The total protein content

151 was determined following the instructions of the RC-DC protein assay (BioRad) and
152 using a standard solution of bovine serum albumin protein (BSA).
153
154 *2.7. Sugar and starch determination*
155 Sugar and starch were measured by anthrone assay with modification [16]. Leaves
156 of every line and WT plants were homogenized with liquid nitrogen, 100 mg of powder
157 were separated and 1 ml of EtOH 80% v/v was added to each sample and the samples
158 were incubated at 80 ºC for 30 min. After heating, the samples were centrifuged 10 min
159 at 10000 rpm and the supernatants were saved. These last steps were conducted three
160 times. For starch extraction, the pellet was dried and then 2 ml of 9.2 N $HClO_4$ were added
161 to analyze the starch content in this extract.
162
163 *2.8. LiHsp83-SAG1 accumulation in transplastomic lines*
164 The analysis of the accumulation of LiHsp83-SAG1 expressed in transplastomic
165 plant was performed as Albarracín et al. [12] with minor modifications. Protein extracts
166 from WT and LiHsp83-SAG1 plants maintained at 25 °C or at 37 °C were separated in a
167 12% SDS-PAGE, transferred onto a PVDF membrane (GE Healthcare) and
168 immunoblotted with an anti-SAG1 polyclonal antibody. A serial dilution (100, 50 and 25
169 ng/μL) of known concentration of an *Escherichia coli*-purified SAG1 protein (Ec-SAG1)
170 was used as the reference. LiHsp83-SAG1 amount was estimated with the Gel-Pro
171 Analyzer software (Media Cybernetics) as described by Albarracín et al. [12]. Page
172 Ruler^{TM} Prestained Protein Ladder (Fermentas) was used as a molecular marker.
173
174 *2.9. RNA isolation and gene expression profiling*

175 Total RNA was isolated from WT and LiHsp83-SAG1 leaves using Trizol reagent
176 (Invitrogen), following the manufacturer's instructions. The RNA concentration and its
177 integrity were analyzed as previously [17]. cDNA was synthesized using oligo dT_{20}
178 (Invitrogen) and M-MLV reverse transcriptase (Promega) according to the manufacturer's
179 instructions. This cDNA was used as a template for Real-Time quantitative PCR (qRT-
180 PCR). The steady-state mRNA levels were analyzed by qRT-PCR as indicated previously
181 [18]. Primer sequences for all the experiments are listed in Supplementary Table S1.
182 Relative quantification was performed by the comparative cycle threshold method. The
183 elongation factor alpha from *Nicotiana tabacum* gene (NtEFα) was used as endogenous
184 control. Reactions were carried out in MicroAmp™ Fast Optical 96-Well Reaction Plate
185 (Thermo Scientific) using the StepOnePlus Real-Time PCR System and the Mx3005P
186 qPCR Software 4.0 (Stratagene). For comparative purposes, relative gene expression was
187 defined with the value of $-Log_2$ in each control plants.
188
189 *2.10. Co-Immunoprecipitation assay*
190 The Co-Immunoprecipitation assay was conducted as Scotti et al. [19] and Inoue
191 et al. [20] with modifications. Briefly, 1 g of LiHsp83-SAG1 leaves exposed at 25 °C or
192 37 °C during 3 weeks were ground in liquid nitrogen and 5 ml of lysis buffer was added
193 (Sucrose 250 mM; Hepes 50 mM, pH 7.2; EDTA 50 mM; DTT 100mM; L-Cistein 6,3
194 mg; MgCl2 1 mM; PVP 0,06 g) and incubated for 1 h at 4 °C. Separately, 20 µL of
195 ProteinA A/G PLUS-Agarose beads (Thermo Fisher) were pre-incubated with 20 µL of
196 anti-LiHsp83 polyclonal sera for 1 h on ice and washed twice with lysis buffer. The
197 extracts were centrifugated at 12000 *g* and 100 µL of each supernatant was incubated with
198 LiHsp83-beads for 4 h at 4 °C. Then, the samples were washed twice with lysis buffer
199 and the beads were separated onto a 12 % 1D-SDS-PAGE. Gels were fixed for 90 minutes

(40% Methanol; 10% glacial acetic acid), stained overnight (10% p/v $(NH_4)_2SO_4$; 2% Orthophosphoric acid; 15 g/L Coomassie brilliant Blue G250; 5% Methanol) and washed with water. 0

2.11. LC-MS/MS

Each lane of the gel was cut into 3 individual pieces. Each band was then cut into 1 mm^3 cube and washed with 50 mM NH_4HCO_3 in 50% CH_3CN. Each group of gel cubes was then dehydrated in CH_3CN for 10 min and dried in a Speed Vac. Protein samples were reduced by dithiothreitol (DTT) and alkylated by iodoacetamide [21]. A solution of 10 ng/µL trypsin in 50 mM NH_4HCO_3 was used to re-swell the gel pieces completely at 4°C for 30 min, followed by a 37°C digestion overnight. A small amount of 10% formic acid was then added to stop the digestion. The sample was then centrifuged at 2,800 x g, and the supernatant was collected for LC-MS/MS.

Two microliters of the tryptic digests were analyzed on the Thermo Q-Exactive plus mass spectrometer coupled to an EASY-nLC 1200 system (Thermo Scientific). Peptides were separated on a fused silica capillary (12 cm x 100 um I.D) packed with Halo C18 (2.7 µm particle size, 90 nm pore size, Michrom Bioresources) at a flow rate of 300 nl/min. Peptides were introduced into the mass spectrometer via a nanospray ionization source at a spray voltage of 2.2 kV. Mass spectrometry data were acquired in a data-dependent top-10 mode, and the lock mass function was activated (m/z, 371.1012; use lock masses, best; lock mass injection, full MS). Full scans were acquired from m/z 350 to 1,600 at 70,000 resolution (automatic gain control [AGC] target, 1^6; maximum ion time [max IT], 100 ms; profile mode). Resolution for dd-MS2 spectra was set to 17,500 (AGC target: 1^5) with a maximum ion injection time of 50 ms. The normalized collision energy was 27 eV. A gradient of 0 to 40% acetonitrile (0.1% FA) over 55 min was applied.

The spectra were searched against the *Nicotiana tabacum* protein database (UP000084051) by Proteome Discoverer (PD) 1.4. The search parameters allowed a 10ppm precursor MS tolerance and a 0.02 Da MS/MS tolerance. Carboxymethylation of cysteines was set up as fixed modifications and Oxidation of methionine (M). Up to two missed tryptic cleavages of peptides were considered with the false-discovery rate set to 1% at the peptide level.

2.12. Statistical analysis

Statistical analysis was carried out with the Prism 5.0 Software (GraphPad) using parametric or non-parametric one-way analysis of variance (ANOVA). Besides, RT-qPCR results were analyzed with fgStatistics (https://sites.google.com/site/fgstatistics/) and permutation test.

3. Results

3.1. Reduced growth and leaf area of LiHsp83-SAG1 plants

In a previous report, we assessed the expression and functionality of *T. gondii* GRA4 and SAG1 antigens and the LiHsp83-SAG1 fusion protein expressed in transplastomic plants [11,12]. In addition, the homoplasmy and correct insertion was demonstrated previously [11,12]. Noticeably, growth retardation was only observed in the LiHsp83-SAG1 line from 20 days after germinating and became more evident when plants were potted in soil (Fig. 1-A, B; Fig S1). Since this phenotype was observed in 4 independent transplastomic lines (Fig. S1), a single line was used in the next experiments. Given this phenotype, the leaf area was measured as a growth parameter. Leaves were photographed, and the images were analyzed to establish the foliar area. The analysis

showed that the leaf area of LiHsp83-SAG1 line was between 5- and 6-fold lower than the other lines and non-transplastomic (WT) plants (Fig. 1-C).

3.2. LiHsp83-SAG1 plants displayed a chlorotic phenotype and very low pigment content

The chlorotic phenotype is the second most evident pleiotropic effect in the LiHsp83-SAG1 line (Fig. 1-B), which could be indicating degradation of photosynthetic pigments, specially chlorophylls [22]. Therefore, chlorophyll (Chl) and accessory pigments content was determined (Fig. 2). SAG1 and GRA4 lines showed no significant differences compared to WT plants in total Chl, Chl *a*, Chl *b* and carotenoids content, while LiHsp83-SAG1 line presented all these pigments significantly diminished compared to WT plants and the other transplastomic lines. Total Chl content of LiHsp83-SAG1 line was 1.6-fold lower than WT plants (Fig. 2-A), while Chl *a* content was 8-fold (Fig. 2-B) and Chl *b* and carotenoids content were 5-fold lower than WT plants (Fig. 2-C, D).

3.3. Very low net photosynthesis and impaired photosystem II in LiHsp83-SAG1 plants

To determine whether the reduction of the foliar area and the decrease of the pigment content observed in LiHsp83-SAG1 plants are correlated with possible damage of the photosynthetic capacity, we evaluated the net photosynthesis (Pn) as a parameter of the normal plant physiology. Not only WT plants but also SAG1 and GRA4 lines showed similar Pn, while LiHsp83-SAG1 plants showed a 22-fold drop compared to WT (Fig. 3). Since the photosynthetic deficiencies could be also related to damage in photosystem II (PSII), the physiological parameters associated to the normal function of PSII were analyzed through the OJIP test (Table 1, Fig. S2). Parameters related to the

PSII efficiency (Fv/Fm and Phi(Eo)) and energy flux (ABS/RC, ETo/RC, and TRo/RC) were analyzed (Table 1; Fig. S2). The two parameters related to PSII efficiency were strongly diminished in the LiHsp83-SAG1 (Table 1). In particular, we evaluated the maximum quantum yield (Fv/Fm) to determine the physiological state of LiHsp83-SAG1 line. The Fv/Fm values for WT, SAG1, and GRA4 plants were normal, while it was remarkably low for LiHsp83-SAG1 plants (Table 1). On the other hand, the analysis of the PSII energy flux parameters in LiHsp83-SAG1 line showed that the apparent antenna size per reaction center (ABS/RC) and trapped energy flux per RC (TRo/RC) are highly increased (Table 1), meanwhile the electron transport flux per RC (ETo/RC), suggesting that functional RC are not frequent in this transplastomic line (Table 1, Fig. S2). Finally, the PI_{ABS} index was measured as a parameter of the global state of the PSII and the lowest values were observed in LiHsp83-SAG1 plants (Table 1).

Once confirmed that the photosynthetic processes are altered in LiHsp83-SAG1 plants, we wondered whether it could be occurring due to a limitation on the CO_2 entrance into the plant cells. To confirm this, the concentration of CO_2 in the substomatal cavity (Ci) and stomatal conductance (g_s) in the three transplastomic lines and WT plants were measured (Fig. 4). The results showed that the CO_2 levels in the stomatal cavity in LiHsp83-SAG1 plants are significantly increased (Fig. 4-A), while no differences in g_s among the three lines and WT plants were observed (Fig. 4-B). According to these results and given the important role of the RuBisCO enzyme in the carbon fixation, relative quantification of RuBisCO in the three transplastomic lines and WT plants was performed (Fig. S3). The relative quantification of the major subunit of RuBisCO (RbcL) showed that LiHsp83-SAG1 plants presented the lowest amount of this subunit (26% of total proteins), while SAG1 and GRA4 lines showed similar RbcL levels contrasted to WT plants (59%, 61% and 65% of total proteins, respectively) (Table 2).

3.4. Reduced levels of total protein, sugars, and starch in LiHsp83-SAG1 plants

Since photosynthetic damage could affect the carbon availability for the proper functioning of other metabolic processes in plant cells, we evaluated the total protein levels, the soluble sugar content and the starch accumulation. SAG1 and GRA4 lines did not show significant differences in comparison to WT plants. On the other hand, the total protein levels were 2.5-fold lower in LiHsp83-SAG1 plants. Although sugars were not able to be detected by this method, the starch content was around 25-fold lower in this transplastomic line, as regards the others (Table 2).

3.5. Transcription of nuclear-encoded photosynthesis-related genes was not altered in LiHsp83-SAG1 plants

To rule out if the pleiotropic effects related to the chlorotic phenotype observed in LiHsp83-SAG1 line are also accompanied by the down-regulation of photosynthesis-related genes, we examined the expression levels of magnesium protoporphyrin chelatase subunit I (*CHLI*), ribulose-1,5-bisphosphate carboxylase/oxygenase small subunit (*RSSU*) and light harvesting chlorophyll a/b binding protein (*LHCa/b*). Interestingly, the expression of *CHLI, RSSU,* and *LHCa/b* genes did not show significant differences between LiHsp83-SAG1 and WT plants (Fig. 5). We also tested the chloroplast heat shock protein (*Hsp90C*) expression levels. Similarly, to the other photosynthesis-related genes, no differences between LiHsp83-SAG1 and WT plants were observed (Fig. 5).

3.6. Heat treatment partially reverts the pleiotropic effects observed in LiHsp83-SAG1 transplastomic line

Since LiHsp83-SAG1 line over-expresses LiHsp83, a member of the family of molecular chaperones, we tested if a heat treatment at 37 °C would improve its

physiological state. After the heat treatment, LiHsp83-SAG1 plants showed an important alleviation of their chlorotic phenotype (Fig. 6-A). Also, leaves of heat-treated LiHsp83-SAG1 plants were bigger than LiHsp83-SAG1 plants raised at 25 °C (Fig. 6-A), their mass (Fresh Weight, FW) was significantly augmented and presented an increment of 8-fold compared to 25 °C (Fig. 6-B). The Pn was also measured and it was greatly improved. At 25 °C, Pn was 22-fold lower than WT (Fig. 3), while at 37 °C it was only 2-fold lower than control (Fig. 6-C), indicating that LiHsp83SAG1 physiology is almost recovered. To verify whether the greening phenotype observed in the LiHsp83-SAG1 line exposed at 37 ºC correlates with a better function of photosynthetic processes, we evaluated the PSII parameters. Interestingly, heat-treated LiHsp83-SAG1 plants showed an evident recovery of the PSII function. Almost all parameters assessed in LiHsp83-SAG1 line at 37 °C were closer to reference values (Fig. 6-D). The maximum quantum yield of primary PSII photochemistry (Fv/Fm) raised up to 0.73 ± 0.01 values, showing a 90% recovery according to non-treated WT plants (Fig. 6-D). Similarly, the apparent antenna size (ABS/RC) in heat-treated LiHsp83-SAG1 plants also showed a significant reduction (3.08 ± 0.54 at 37 ºC vs. 12.34 ± 3.06 at 25 ºC), suggesting an increment in the number of functional reaction centers. Finally, the PI_{ABS} index was measured and the heat-treated plants belonging to the LiHsp83-SAG1 line showed a strong recovery of this value (0.72 ± 0.09 at 37 ºC vs. 0.01 ± 0.007 at 25 ºC); although it did not reach the levels of the non-heated WT plants (3.50 ± 1.13). It should be mentioned that the heat treatment produced a delay in the growth of WT plants (Fig. S4), however it did not alter any of the parameters measured in the WT plants at 37 ºC compared to WT at 25 ºC (Fig. 6-D). To determine whether the recovery of the PSII parameters in heat-treated LiHsp83-SAG1 plants is due to changes in the expression of photosynthesis-related genes, the levels of *Hsp90C, LHCa/b, CHLI* and *RSSU* genes were measured (Fig. 7). In particular, *Hsp90C* and

LHCa/b expression did not show differences at 37 °C along the time. After 1 week of heat treatment, *Hsp90C* expression tends to be upregulated in WT plants compared to LiHsp83-SAG1 plants, but no significant differences were observed (Fig. 7-A). Besides, after 3 weeks of heat treatment, *LHCa/b* expression showed a tendency to be down-regulated, but there were no differences with WT plants (Fig. 7-B). On the other hand, the *CHLI* and *RSSU* expression were down-regulated in heat-treated LiHsp83-SAG1 line and WT plants, but it was only significantly different in LiHsp83-SAG1 line after the 3 weeks-treatment (Fig. 7-C, D). Regarding the total protein content, there was an increase in heat-treated LiHsp83-SAG1 plants compared to those non-treated (Fig. 8-A). More importantly, a significant increase in the relative RbcL content in heat-treated LiHsp83-SAG1 plants reaching similar levels to those obtained in non-heated WT plants was observed (Fig. 8-B). On the other hand, no differences of RbcL accumulation between heat- and non-heat-treated WT plants were detected (Fig. S2, Fig. 8-B).

In an attempt to find the reason why the reversion phenotype of the LiHsp83-SAG1 line at 37 °C, we performed a co-immuno precipitation (CO-IP) assay using anti-LiHsp83 polyclonal antisera (Table S3). Surprisingly, LiHsp83-SAG1 is interacting with key photosynthesis-related proteins at 37 °C, while at 25 °C is not. Among the critical interactors we found Ribulose bisphosphate carboxylase large chain (Accession number in UniProt database: A0A140G1S3), Ribulose bisphosphate carboxylase small chain (A0A1S3YB15, Q84QE5), Ribulose bisphosphate carboxylase/oxygenase activase (A0A1S4AKW3), Chlorophyll a-b binding protein (A0A1S3YAU9, A0A1S4CEW8, A0A1S3YPE9), oxygen-dependent coproporphyrinogen-III oxidase (A0A1S3XMU0) and ATP synthase subunit alpha (A0A140G1P7).

3.7. Heat treatment improves the LiHsp83-SAG1 yield

374 Finally, the accumulation of LiHsp83-SAG1 protein from heat-treated
375 transplastomic plants was evaluated by Western blot (Fig. 8-C). The yield of LiHsp83-
376 SAG1 obtained in transplastomic plants raised at 25 °C was approximately 2.4 µg per
377 gram of FW. In contrast, LiHsp83-SAG1 accumulation in heat-treated plants was around
378 1 µg per gram of FW (Fig. 8-C). However, as the heat treatment produced larger LiHsp83-
379 SAG1 plants, a yield improvement equivalent to 5-7 mg of LiHsp83-SAG1 per plant (Fig.
380 8-D) was observed.
381
382 **4. Discussion**
383 LiHsp83-SAG1 overexpression in transplastomic plants led to pleiotropic effects,
384 such as chlorosis, reduced RbcL content and growth retardation [12]; and this phenotype
385 could limit the ability to produce the protein of interest. In this study, we performed an
386 integrated analysis of the metabolism and the photosynthetic parameters of these plants,
387 together with the assessment of the LiHsp83-SAG1 line response to a heat treatment.
388
389 *4.1. Photosynthesis process is damaged in the LiHsp83-SAG1 line*
390 Over-expression of transgenes in chloroplasts often leads to detrimental effects on
391 chloroplast development and photosynthesis. The green color of chloroplasts is due to
392 photosynthetic pigments which are associated with electron transfer proteins and all
393 together form the antenna complex [23]. This pigment-protein complex is able to collect
394 the light energy, transfer it to the reaction centers (RC) and use it for plant biomass
395 production [24]. Therefore, growth retardation and chlorosis phenotype are linked to the
396 chlorophylls and carotenoids disposal and the reduced photosynthesis capacity [10]. In
397 this study, we analyzed three transplastomic lines, but we observed that only LiHsp83-
398 SAG1 line present such phenotype and we determined that the photosynthetic processes

399 are damaged. We first hypothesized that the expression levels reached for the LiHsp83-
400 SAG1 line were toxic for plant metabolism. Although LiHsp83-SAG1 protein
401 accumulation is not superior to 3% of the TSP, it has been reported that a wide range of
402 heterologous production is able to lead deleterious effects. As it was reported by others,
403 an exceptional production of exogenous protein (up to 70 % of total soluble proteins
404 (TSP)), intermediate production (18 % of TSP) or as little as 0.2 % of TSP have led to
405 chlorosis and growth retardation, without affecting flowering and seed setting [19,25–
406 27]. On the other hand, accumulation of 2 % of TSP, not only led to chlorosis and growth
407 retardation but also produced male sterility in all transplastomic lines studied [8]. When
408 the transgene overburdens the chloroplast expression machinery, a poisoning of the
409 endogenous gene expression occurs, and it would lead to such phenotype. Several studies
410 showed that over-expression of recombinant proteins in chloroplasts is usually
411 accompanied by a significant reduction in the accumulation of plastid-encoded proteins,
412 most notably the accumulation of the RuBisCO large (RbcL) and small (RSSU) subunits
413 because of a diminish of transcription rate of endogenous genes [26,27]. Since pale plants
414 contain reduced RbcL protein, we aimed to determine whether the low RbcL
415 accumulation observed in LiHsp83-SAG1 line is due to a decrease of its gene expression.
416 We evaluated the levels of *RSSU* and other photosynthesis-related genes, but
417 unexpectedly, none of the genes studied in LiHsp83-SAG1 plants showed statistic
418 differences compared to WT plants. The results showed that the RSSU mRNA levels do
419 not correlate with the low levels of RbcL protein accumulated, though stable RSSU
420 mRNA level does not preclude an effect on the accumulation and translation of the RbcL
421 mRNA. Likewise, there was no significant down-regulation of *LHCa/b* and *CHL1* genes
422 as it was expected given the reduction of Chl *a* and Chl *b* pigments previously observed.
423 These findings are consistent with other studies carried out by Waheed et al. [8]. They

demonstrated that even though recombinant protein yields obtained were under to 2%, the chlorosis effects were directly related with the presence of the recombinant protein. This suggests that the presence of the recombinant protein would modify the chloroplast metabolism affecting photosynthetic mechanisms and, in consequence, the correct plant development [10]. We believe that the reduction of RuBisCO amount in LiHsp83-SAG1 line was probably due to an impairment of photosynthesis.

The significance of Hsp90C for chloroplast biogenesis has been previously reported [20,28,29]. In fact, the lack of Hsp90C in chloroplasts either by Hsp90C co-suppression, by a point mutation in Hsp90C or Hsp90C silencing by VIGS displayed a yellow-green phenotype and impaired growth in Arabidopsis as well as in tobacco [28–32]. Considering that LiHsp83-SAG1 is constitutively over-expressed in chloroplasts and bearing in mind that LiHsp83 shares a 65 % of similarity with *N. tabacum* Hsp90C, we considered the possibility that the accumulation of Hsp90C might be impeded due to the high expression levels of the recombinant protein. To rule out this possibility, we examined the expression levels of *Hsp90C* gene, and it did not present significant differences between LiHsp83-SAG1 and WT plants. Therefore, we can conclude that overexpression of LiHsp83-SAG1 is not disturbing endogenous *Hsp90C* gene expression. Other studies associated the impairment of plastid development to the carbohydrate-binding activity of the recombinant protein or to the binding of the recombinant protein to thylakoids [33,34]. Since no putative thylakoid- or carbohydrate-binding motifs were identified in the LiHsp83-SAG1 sequence, our results support the idea that the expression of LiHsp83-SAG1 protein could be affecting the amount of RuBisCO and/or other proteins involved in photosynthetic processes rather than affecting the transcription rate of photosynthesis-related genes or the plastid development due to its binding to thylakoids.

449 *4.2. Heat treatment partially reverts the pleiotropic effects observed in LiHsp83-SAG1*
450 *transplastomic line*

451 Unlike most chaperones, Hsp90s are constitutively expressed at much higher
452 concentrations than required to fulfill their normal functions and they are essential
453 proteins required for the growth of cells at high temperatures [35,36]. Considering this,
454 we aimed to know whether LiHsp83-SAG1 line which has higher levels of Hsp90 since
455 over-expresses LiHsp83 would improve its fitness at 37 °C. Interestingly, LiHsp83-SAG1
456 plants showed a partial alleviation of their phenotype. They grew greener and bigger, their
457 Fv/Fm was close to WT and RbcL protein amount increased. The explanation for this
458 could be that Hsp90s are induced by heat shock and Hsp90 network facilitates the
459 adaptation to new environments [37]. As endogenous Hsp90C are also induced by heat
460 shock [29,31,38], we first evaluated if the Hsp90C mRNA was newly synthesized after
461 the heat treatment. Besides, we assessed whether the reason of the phenotype alleviation
462 was due to an up-regulation of *RSSU* and/or other photosynthetic-related genes. The
463 results demonstrated that there were no differences in *Hsp90C* expression between
464 LiHsp83-SAG1 heat-treated plants and WT heat-treated plants. On the other hand, *CHLI*
465 and *RSSU* expression were down-regulated in LiHsp83-SAG1 plants. Similar to observed
466 previously, the higher RbcL accumulation and the improvement of photosynthesis after
467 heat treatment do not correlate with gene expression. Therefore, we hypothesize that as
468 LiHsp83 is a heat shock protein, the excess of this molecular chaperone benefits the plant
469 in a possible heat shock and prevents the expected denaturation of proteins. Some reports
470 showed that the heterologous expression of Hsp90 proteins was demonstrated to be
471 beneficial for the organism expressing them [37,39,40]. For instance, *Escherichia coli*
472 showed enhanced thermotolerance by expressing heterologous rice Hsp90 (OsHsp90)
473 [39]. Besides, Hsp90.3 isoform from *Arabidopsis thaliana* supported the yeast growth

474 under heat stress [40]. Moreover, when *Saccharomyces cerevisiae* Hsp90 was replaced
475 by an ortholog from *Yarrowia lipolytica*, yeasts exhibited an improved growth in
476 hypersaline environments [37]. In this context, we conducted a co-immunoprecipitation
477 assay to investigate the interactors of LiHsp83-SAG1 protein at 37 °C. We found that
478 LiHsp83-SAG1 is interacting with remarkable proteins involved in photosynthesis, like
479 RSSU, RbcL, RuBisCO activase, Chlorophyll a/b binding protein, ATP synthase subunit
480 alpha and oxygen-dependent coproporphyrinogen-III oxidase suggesting that LiHsp83-
481 SAG1 present in stroma could bind to these key proteins chaperoning and/or stabilizing
482 their structures during the heat treatment. However, further studies should be done to shed
483 light on the interaction among LiHsp83-SAG1 and those proteins. Finally, several
484 approaches were explored to reduce the pleiotropic effect in transplastomic plants in order
485 to increase the recombinant proteins yields [26,41,42]. In our study, the heat treatment
486 applied help LiHsp83-SAG1 plants to alleviate their phenotype, although the LiHsp83-
487 SAG1 content was weakly decreased in heat treatment (1 μg per g FW at 37 ºC vs 2.4 μg
488 per g FW at 25 ºC). In this context, we cannot rule out that the alleviation observed of the
489 phenotype may be due by a reduction of the accumulation levels of the recombinant
490 protein at 37 ºC. In conclusion, the results described here suggest that the pleiotropic
491 effect observed in the LiHsp83-SAG1 plants are mainly due to a misfunction of the PSII
492 and a significant reduction of RbcL abundance. In addition, we demonstrated that heat
493 stress alleviates the phenotype of this transplastomic line suggesting that this strategy
494 could help us to discern, in future experiments, the specific mechanisms that would be
495 influencing the metabolic and photosynthetic processes under this condition. As far as we
496 know, this is the first report where demonstrated that a transplastomic line performs much
497 better at higher temperatures.
498

Acknowledgments

We would like to thank Patricia A. Uchiya (CIC, Buenos Aires) for her technical support. This work was supported by grants from the Agencia Nacional de Promoción Científica y Tecnológica of Argentina (PICT: 2014-3473, 2016-0113 and 2016-0621). This study also received institutional support from the Universidad Nacional General de San Martín (UNSAM, Argentina). The Vermont Genetics Network Proteomics Facility is supported through NIH grant P20GM103449 from the INBRE Program of the National Institute of General Medical Sciences.

References

[1] J. Buyel, Process Development Strategies in Plant Molecular Farming, Curr. Pharm. Biotechnol. 16 (2015) 966–982. doi:10.2174/1389201016111509021154 13.

[2] M.K. Mandal, H. Ahvari, S. Schillberg, A. Schiermeyer, Tackling Unwanted Proteolysis in Plant Production Hosts Used for Molecular Farming, Front. Plant Sci. 7 (2016) 1–6. doi:10.3389/fpls.2016.00267.

[3] M. Tschofen, D. Knopp, E. Hood, E. Stöger, Plant Molecular Farming: Much More than Medicines, Annu. Rev. Anal. Chem. 9 (2016) 271–294. doi:10.1146/annurev-anchem-071015-041706.

[4] N. Ahmad, F. Michoux, A.G. Lössl, P.J. Nixon, Challenges and perspectives in commercializing plastid transformation technology, J. Exp. Bot. 67 (2016) 5945–5960. doi:10.1093/jxb/erw360.

[5] M. Adem, D. Beyene, T. Feyissa, Recent achievements obtained by chloroplast transformation, Plant Methods. 13 (2017) 1–11. doi:10.1186/s13007-017-0179-1.

[6] H. Daniell, C.-S. Lin, M. Yu, W.-J. Chang, Chloroplast genomes: diversity, evolution, and applications in genetic engineering, Genome Biol. 17 (2016) 134. doi:10.1186/s13059-016-1004-2.

[7] R. Bock, Engineering Plastid Genomes: Methods, Tools, and Applications in Basic Research and Biotechnology, Annu. Rev. Plant Biol. 66 (2015) 211–241. doi:10.1146/annurev-arplant-050213-040212.

[8] M.T. Waheed, N. Thönes, M. Müller, S.W. Hassan, J. Gottschamel, E. Lössl, H.P. Kaul, A.G. Lössl, Plastid expression of a double-pentameric vaccine candidate containing human papillomavirus-16 l1 antigen fused with ltb as adjuvant: Transplastomic plants show pleiotropic phenotypes, Plant Biotechnol. J. 9 (2011) 651–660. doi:10.1111/j.1467-7652.2011.00612.x.

[9] N. Scotti, L. Sannino, A. Idoine, P. Hamman, A. De Stradis, P. Giorio, L. Maréchal-Drouard, R. Bock, T. Cardi, The HIV-1 Pr55gagpolyprotein binds to plastidial membranes and leads to severe impairment of chloroplast biogenesis and seedling lethality in transplastomic tobacco plants, Transgenic Res. 24 (2015) 319–331. doi:10.1007/s11248-014-9845-5.

[10] N. Scotti, T. Cardi, Transgene-induced pleiotropic effects in transplastomic plants, Biotechnol. Lett. 36 (2014) 229–239. doi:10.1007/s10529-013-1356-6.

[11] M. Del L. Yácono, I. Farran, M.L. Becher, V. Sander, V.R. Sánchez, V. Martín, J. Veramendi, M. Clemente, A chloroplast-derived Toxoplasma gondii GRA4 antigen used as an oral vaccine protects against toxoplasmosis in mice, Plant Biotechnol. J. 10 (2012) 1136–1144. doi:10.1111/pbi.12001.

[12] R.M. Albarracín, M.L. Becher, I. Farran, V.A. Sander, M.G. Corigliano, M.L. Yácono, S. Pariani, E. Sánchez López, J. Veramendi, M. Clemente, The fusion of

547 Toxoplasma gondii SAG1 vaccine candidate to Leishmania infantum heat shock
548 protein 83-kDa improves expression levels in tobacco chloroplasts, Biotechnol. J.
549 10 (2015) 748–759. doi:10.1002/biot.201400742.

550 [13] D.R. Hoagland, D.I. Arnon, The water-culture method for growing plants without
551 soil, Calif. Agric. Exp. Stn. Circ. 347 (1950) 1–32. doi:citeulike-article-
552 id:9455435.

553 [14] F.W. Lichtenthaler, Karl Freudenberg, Burckhardt Helferich, Hermann O. L.
554 Fischer: A centennial tribute, Carbohydr. Res. 164 (1987) 1–22.

555 [15] R.J. Strasser, A. Srivastava, M. Tsimilli-Michael, The fluorescence transient as a
556 tool to characterize and screen photosynthetic samples, 2000.
557 http://ww.hansatech-instruments.com/docs/the fluorescence transient.pdf.

558 [16] S. Yoshida, D.A. Forni, J.H. Cock, K.A. Gomez, Measurement of leaf area, leaf
559 area index, and leaf thickness, Lab. Man. Physiol. Stud. Rice. (1976) 69–72.

560 [17] M.G. Corigliano, A. Maglioco, M. Laguía Becher, A. Goldman, V. Martín, S.O.
561 Angel, M. Clemente, Plant Hsp90 proteins interact with B-cells and stimulate
562 their proliferation., PLoS One. 6 (2011) e21231.
563 doi:10.1371/journal.pone.0021231.

564 [18] S. Pariani, M. Contreras, F.R. Rossi, V. Sander, M.G. Corigliano, F. Simón, M.
565 V. Busi, D.F. Gomez-Casati, F.L. Pieckenstain, V.G. Duschak, M. Clemente,
566 Characterization of a novel Kazal-type serine proteinase inhibitor of Arabidopsis
567 thaliana, Biochimie. 123 (2016) 85–94. doi:10.1016/j.biochi.2016.02.002.

568 [19] N. Scotti, F. Alagna, E. Ferraiolo, G. Formisano, L. Sannino, L. Buonaguro, A.
569 De Stradis, A. Vitale, L. Monti, S. Grillo, F.M. Buonaguro, T. Cardi, High-level

570 expression of the HIV-1 Pr55gag polyprotein in transgenic tobacco chloroplasts,
571 Planta. 229 (2009) 1109–1122. doi:10.1007/s00425-009-0898-2.

572 [20] H. Inoue, M. Li, D.J. Schnell, An essential role for chloroplast heat shock protein
573 90 (Hsp90C) in protein import into chloroplasts, Proc. Natl. Acad. Sci. 110
574 (2013) 3173–3178. doi:10.1073/pnas.1219229110.

575 [21] P.C. Spiess, B. Deng, R.J. Hondal, D.E. Matthews, V. van del Vilet, Proteomic
576 profilling of acrolein adducts in human lung epitelial cells, J. Proteomics. 74
577 (2011) 2380–2394. doi:10.1016/j.jprot.2011.05.039.Proteomic.

578 [22] V.I. Deltoro, A. Calatayud, F. Morales, A. Abadía, E. Barreno, Changes in net
579 photosynthesis , chlorophyll fluorescence and xanthophyll cycle interconversions
580 during freeze-thaw cycles in the Mediterranean moss Leucodon sciuroides,
581 Oecologia. 120 (1999) 499–505.

582 [23] A.K. Biswal, G.K. Pattanayak, S.S. Pandey, S. Leelavathi, V.S. Reddy,
583 Govindjee, B.C. Tripathy, Light Intensity-Dependent Modulation of Chlorophyll
584 b Biosynthesis and Photosynthesis by Overexpression of Chlorophyllide a
585 Oxygenase in Tobacco, Plant Physiol. 159 (2012) 433–449.
586 doi:10.1104/pp.112.195859.

587 [24] N. Msilini, J. Essemine, M. Zaghdoudi, J. Harnois, M. Lachaâl, Z. Ouerghi, R.
588 Carpentier, How does iron deficiency disrupt the electron flow in photosystem I
589 of lettuce leaves?, J. Plant Physiol. 170 (2013) 1400–1406.
590 doi:10.1016/j.jplph.2013.05.004.

591 [25] G. Tissot, H. Canard, M. Nadai, A. Martone, J. Botterman, M. Dubald,
592 Translocation of aprotinin, a therapeutic protease inhibitor, into the thylakoid
593 lumen of genetically engineered tobacco chloroplasts, Plant Biotechnol. J. 6

(2008) 309–320. doi:10.1111/j.1467-7652.2008.00321.x.

[26] M. Oey, M. Lohse, B. Kreikemeyer, R. Bock, Exhaustion of the chloroplast protein synthesis capacity by massive expression of a highly stable protein antibiotic, Plant J. 57 (2009) 436–445. doi:10.1111/j.1365-313X.2008.03702.x.

[27] M.M. Rigano, C. Manna, A. Giulini, E. Pedrazzini, M. Capobianchi, C. Castilletti, A. Di Caro, G. Ippolito, P. Beggio, C. De Giuli Morghen, L. Monti, A. Vitale, T. Cardi, Transgenic chloroplasts are efficient sites for high-yield production of the vaccinia virus envelope protein A27L in plant cells, Plant Biotechnol. J. 7 (2009) 577–591. doi:10.1111/j.1467-7652.2009.00425.x.

[28] D. Cao, J.E. Froehlich, H. Zhang, C.L. Cheng, The chlorate-resistant and photomorphogenesis-defective mutant cr88 encodes a chloroplast-targeted HSP90, Plant J. 33 (2003) 107–118. doi:10.1046/j.1365-313X.2003.016011.x.

[29] J. Feng, P. Fan, P. Jiang, S. Lv, X. Chen, Y. Li, Chloroplast-targeted Hsp90 plays essential roles in plastid development and embryogenesis in Arabidopsis possibly linking with VIPP1, Physiol. Plant. 150 (2014) 292–307. doi:10.1111/ppl.12083.

[30] Y. Lin, C.L. Cheng, A chlorate-resistant mutant defective in the regulation of nitrate reductase gene expression in Arabidopsis defines a new HY locus, Plant Cell. 9 (1997) 21–35. doi:10.1105/tpc.9.1.21\r9/1/21 [pii].

[31] S.E. Oh, C. Yeung, R. Babaei-Rad, R. Zhao, Cosuppression of the chloroplast localized molecular chaperone HSP90.5 impairs plant development and chloroplast biogenesis in Arabidopsis, BMC Res. Notes. 7 (2014) 1–15. doi:10.1186/1756-0500-7-643.

[32] S.A. Bhor, C. Tateda, T. Mochizuki, K.T. Sekine, T. Yaeno, N. Yamaoka, M.

Nishiguchi, K. Kobayashi, Inducible transgenic tobacco system to study the mechanisms underlying chlorosis mediated by the silencing of chloroplast heat shock protein 90, VirusDisease. 28 (2017) 81–92. doi:10.1007/s13337-017-0361-0.

[33] K. Petersen, R. Bock, High-level expression of a suite of thermostable cell wall-degrading enzymes from the chloroplast genome, Plant Mol. Biol. 76 (2011) 311–321. doi:10.1007/s11103-011-9742-8.

[34] D. Castiglia, L. Sannino, L. Marcolongo, E. Ionata, R. Tamburino, A. De Stradis, B. Cobucci-Ponzano, M. Moracci, F. La Cara, N. Scotti, High-level expression of thermostable cellulolytic enzymes in tobacco transplastomic plants and their use in hydrolysis of an industrially pretreated Arundo donax L. biomass, Biotechnol. Biofuels. 9 (2016) 1–16. doi:10.1186/s13068-016-0569-z.

[35] K. a Borkovich, F.W. Farrelly, D.B. Finkelstein, J. Taulien, S. Lindquist, Hsp82 Is an Essential Protein That Is Required in Higher Concentrations for Growth of Cells At Higher Temperatures., Mol. Cell. Biol. 9 (1989) 3919–30. http://www.pubmedcentral.nih.gov/articlerender.fcgi?artid=362454&tool=pmcentrez&rendertype=abstract.

[36] D.F. Jarosz, S. Lindquist, Hsp90 and environmental stress transform the adaptive value of natural genetic variation., Science. 330 (2010) 1820–4. doi:10.1126/science.1195487.

[37] T.C.-T. Koubkova-Yu, J.-C. Chao, J.-Y. Leu, Heterologous Hsp90 promotes phenotypic diversity through network evolution, PLOS Biol. 16 (2018) e2006450. doi:10.1371/journal.pbio.2006450.

[38] F. Willmund, M. Schroda, HEAT SHOCK PROTEIN 90C is a bona fide Hsp90

641 that interacts with plastidic HSP70B in Chlamydomonas reinhardtii., Plant
642 Physiol. 138 (2005) 2310–2322. doi:10.1104/pp.105.063578.

643 [39] D. Liu, Z. Lu, Z. Mao, S. Liu, Enhanced thermotolerance of E. coli by expressed
644 OsHsp90 from rice (Oryza sativa L.), Curr. Microbiol. 58 (2009) 129–133.
645 doi:10.1007/s00284-008-9288-4.

646 [40] X. Xu, H. Song, Z. Zhou, N. Shi, Q. Ying, H. Wang, Functional characterization
647 of AtHsp90.3 in Saccharomyces cerevisiae and Arabidopsis thaliana under heat
648 stress., Biotechnol. Lett. 32 (2010) 979–87. doi:10.1007/s10529-010-0240-x.

649 [41] R. Sanz-Barrio, A.F.S. Millán, P. Corral-Martínez, J.M. Seguí-Simarro, I. Farran,
650 Tobacco plastidial thioredoxins as modulators of recombinant protein production
651 in transgenic chloroplasts, Plant Biotechnol. J. 9 (2011) 639–650.
652 doi:10.1111/j.1467-7652.2011.00608.x.

653 [42] J.S. Tregoning, P. Nixon, H. Kuroda, Z. Svab, S. Clare, F. Bowe, N. Fairweather,
654 J. Ytterberg, K.J. van Wijk, G. Dougan, P. Maliga, Expression of tetanus toxin
655 Fragment C in tobacco chloroplasts, Nucleic Acids Res. 31 (2003) 1174–1179.
656 doi:10.1093/nar/gkg221.

657

658 **Legends of figures**

659 **Fig. 1.** Phenotype characterization of transplastomic lines. (A) Twenty-days-old after
660 germination in MS medium. (B) Forty-days-old after germination of non-transformed
661 (WT) plants and SAG1, GRA4 and LiHsp83-SAG1 transplastomic lines grown in sterile
662 sand: soil: perlite mixture. **c** Leaf area analysis. The area of the youngest fully developed
663 leaf from 40-days-old plants was calculated with Gel-Pro Analyzer software. Results are
664 the mean of 10 biological replicates ± SEM. Statistical analysis was performed by one-

665 way non-parametric analysis of variance (ANOVA) using the Dunn's multiple
666 comparison test. LiHsp83-SAG1 vs WT, SAG1 and GRA4: ** $p < 0.01$.
667
668 **Fig. 2.** Chlorophyll (Chl) and accessory pigments content in the transplastomic lines. (A)
669 Total Chl, (B) Chl *a*, (C) Chl *b,* (D) Carotenoids present in the youngest fully developed
670 leaf in 40-days-old plants were determined. Non-transformed (WT) plants and SAG1,
671 GRA4 and LiHsp83-SAG1 transplastomic lines were assessed. Results are the mean of
672 10 biological replicates ± SEM. Statistical analysis was performed by Kruskal-Wallis
673 analysis using the Dunn's multiple comparison test. WT vs LiHsp83-SAG1: ** $p < 0.01$.
674
675 **Fig. 3.** Determination of net photosynthesis (Pn). Pn was measured in the youngest
676 completely developed leaf at light saturation. Results are the mean of 6 biological
677 replicates ± SEM. Statistical analysis was performed by Kruskal-Wallis analysis using
678 the Dunn's multiple comparison test. LiHsp83-SAG1 vs WT, SAG1 and GRA4: * $p <$
679 0.05.
680
681 **Fig. 4.** Gas Exchange determination in the transplastomic lines. (A) Concentration of CO_2
682 in the substomatal cavity (C_i). (B) stomatal conductance (g_s). Ci and g_s were measured in
683 the youngest completely developed leaf at light saturation. Results are the mean of 6
684 biological replicates ± SEM. Statistical analysis was performed by Kruskal-Wallis
685 analysis using the Dunn's multiple comparison test. LiHsp83-SAG1 vs WT, SAG1 and
686 GRA4: * $p < 0.05$.
687
688 **Fig. 5.** Analysis of the expression profile of photosynthesis- and heat-related genes. qRT-
689 PCR was used to analyze the abundance of CHLI; RSSU; LHCa/b; Hsp90C transcripts

690 in the LiHsp83-SAG1 plants. The transcript levels were normalized to WT transcript
691 level. *NtEFα* gene was used as an internal control. Three technical replicates were
692 performed per experiment, and three independent experiments were performed. The
693 expression analysis was assessed in 47-day-old plants.
694
695 **Fig. 6.** Analysis of the reversion of pleiotropic phenotype in 60-days-old LiHsp83-SAG1
696 plants. (A) Image of LiHsp83-SAG1 plants grown at 25 °C or 37 °C for 3 weeks. (B)
697 Aerial mass of LiHsp83-SAG1 plants grown at 25 °C (grey bar) or heat-treated at 37 °C
698 for 3 weeks (black bar). Results are the mean of 10 biological replicates ± SEM. Statistical
699 analysis was performed using the unpaired t-test with Welch's correction. **** $p <$
700 0.0001. (C) Quantification of the net photosynthesis (Pn) in WT and LiHsp83-SAG1 heat-
701 treated plants at 37 ºC for 3 weeks. Pn was measured in the youngest completely
702 developed leaf at light saturation. Statistical analysis was performed using Mann-Whitney
703 test. (D) Analysis of photosynthetic parameters in WT and LiHsp83-SAG1 plants grown
704 at 25 °C or 37 °C for 3 weeks. Mean values of 8 OJIP parameters are shown in radar
705 charts for WT at 25 °C (grey dotted line), LiHsp83-SAG1 at 25 °C (grey solid line) and
706 LiHsp83-SAG1 at 37 °C (black solid line). Results are expressed as relative to WT, which
707 was assigned to 1. The definition of each parameter is provided in Table S2.
708
709 **Fig. 7.** Analysis of the expression profile of photosynthesis- and heat-related genes. qRT-
710 PCR was used to analyze the abundance of (A) Hsp90C; (B) LHCa/b; (C) RSSU; (D)
711 CHLI transcripts in WT and LiHsp83-SAG1 plants exposed at 37 °C for 1 week (1w) or
712 3 weeks (3w). The transcript levels at 37 ºC were normalized to transcript level at 25 ºC.
713 *NtEFα* gene was used as an internal control. Three technical replicates were performed

per experiment, and three independent experiments were performed. The expression analysis was assessed in 60-day-old WT and LiHsp83-SAG1 plants. **p < 0.01.

Fig. 8. Analysis of the heat treatment effect on WT and LiHsp83-SAG1 plants. (A) Content of total protein in WT and LiHsp83-SAG1 plants maintained either at 25 °C, 37 °C 1 week (1w) or 37 °C 3 week (3w) quantified by RC-DC method. Statistical analysis was performed by one-way analysis of variance (ANOVA) using the Bonferroni's Multiple Comparison Test. LiHsp83-SAG1 25 ºC vs LiHsp83-SAG1 37 ºC 1w and 3w. *** p < 0.001; **** p < 0.0001. (B) Analysis of RbcL protein in WT and LiHsp83-SAG1 grown at 37 ºC for 1w or 3w. Total soluble proteins (25 µg) extracted from WT or LiHsp83-SAG1 plants electrophoresed on SDS-PAGE gels and stained with Coomassie brilliant blue. Arrow points Ribulose bisphosphate carboxylase large subunit (RbcL). (C) Quantification of LiHsp83-SAG1 by Western blot analysis in 60-days-old transplastomic plants grown at 37 ºC for 3 weeks. Ten micrograms of total protein extracts from WT and LiHsp83-SAG1 plants maintained at 25 °C or at 37 °C for 3 weeks (3w) were immunoblotted with an anti-SAG1 polyclonal antibody. Serial dilution of rSAG1 (100, 50, 25 and 12.5 ng/µl) was used as reference [12]. (D) Estimation of LiHsp83-SAG1 yields per plant. Results are the mean of 4 biological replicates ± SEM. Statistical analysis was performed using unpaired t test with Welch's correction. *** p < 0.001.

Supplementary material

Fig. S1. Phenotype of a wild-type (WT) tobacco plant and 4 independent transplastomic lines of LiHsp83-SAG1 grown for 8 weeks in a phytotron at 25 ºC and 16 h day/ 8 h night photoperiod.

Fig. S2. Photosynthetic characterization of transplastomic lines. Photosynthetic parameters of 40-days-old WT plants and transplastomic lines were measured. Mean values of 8 OJIP parameters are shown in radar charts for WT (grey solid line), SAG1 (black dotted line), GRA4 (grey dotted line) and LiHsp83-SAG1 (black solid line). Results are expressed as relative to WT, which was assigned to 1. The definition of each parameter is provided in table S2.

Fig. S3. Expression of the Ribulose bisphosphate carboxylase large subunit (RbcL). Total protein extracts (25 µg) from WT plants or SAG1, GRA4 and LiHsp83-SAG1 lines were analyzed by Coomassie blue-stained SDS-PAGE gel. Star points RbcL and arrow points LiHsp83-SAG1 fusion protein.

Fig. S4. Phenotype of a wild-type (WT) tobacco plants grown for 8 weeks in a phytotron at 25 ºC (WT 25 ºC) and plants grown for 5 weeks at 25 °C and heat stresses in a phytotron at 37 °C for 3 weeks (WT 37 ºC).

Table 1

Analysis of PSII efficiency (Fv/Fm and Phi(Eo)), energy flux (ABS/RC, ETo/RC, TRo/RC) and PSII global state (PI_{ABS}) parameters.

LINES	Fv/Fm	Phi(Eo)	ABS/RC	TRo/RC	PI_{ABS}
WT	0.824 ± 0.003^{a}	0.405 ± 0.006^{a}	1.81 ± 0.03^{a}	0.502 ± 0.02^{a}	2.524 ± 0.129^{a}
GRA4	0.808 ± 0.012^{a}	0.327 ± 0.009^{a}	2.18 ± 0.11^{a}	0.482 ± 0.01^{a}	1.258 ± 0.198^{a}
SAG1	0.773 ± 0.008^{a}	0.303 ± 0.007^{a}	2.37 ± 0.06^{a}	0.474 ± 0.02^{a}	1.014 ± 0.072^{a}
LiHsp83-SAG1	0.199 ± 0.007^{b}	0.021 ± 0.003^{b}	16.89 ± 0.59^{b}	1.083 ± 0.08^{b}	0.002 ± 0.001^{b}

Results are expressed as the mean ± SD. Statistical analysis was performed by Kruskal-Wallis analysis using the Dunn's multiple comparison test. Different letters indicate a significance of 0.05. Ten plants from each line were used.

Table 2

Content of RbcL, total proteins, soluble sugars and starch.

LINES	PROTEINS		SUGARS	
	RbcL relative levels (% RbcL band / total bands)	Total proteins (mg g^{-1} FW)	Soluble Sugars (mg g^{-1} FW)	Starch (mg Glc g^{-1} FW)
WT	65.71	11.72 ± 0.89^{a}	9.24 ± 1.34^{a}	84.53 ± 11.84^{a}
GRA4	60.85	9.05 ± 0.74^{a}	7.95 ± 1.34^{a}	82.93 ± 11.64^{a}
SAG1	59.27	9.45 ± 0.59^{a}	6.62 ± 2.02^{a}	78.02 ± 13.33^{a}
LiHsp83-SAG1	26.17	4.17 ± 0.25^{b}	*Non-detectable*	3.91 ± 1.27^{b}

Results are expressed as the mean ± SD. Statistical analysis was performed by Kruskal-Wallis analysis using the Dunn's multiple comparison test. Different letters indicate a significance of 0.05. Ten plants from each line were used.

Fig. 1

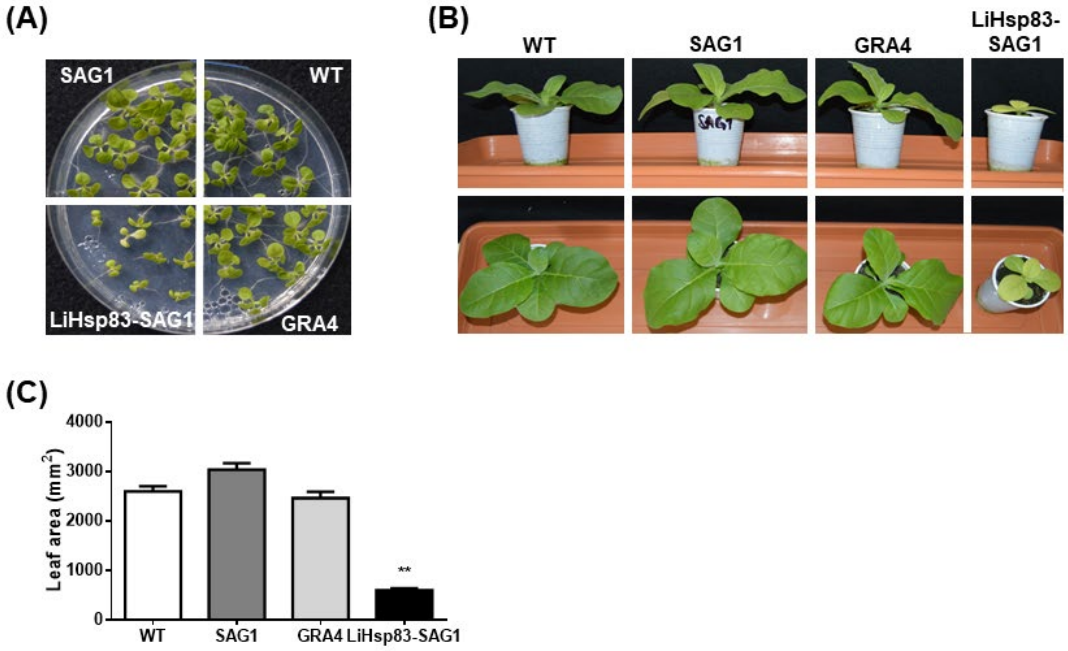
(A)
SAG1
WT
LiHsp83-SAG1
GRA4
(B)
WT
SAG1
GRA4
LiHsp83-SAG1
(C)
Leaf area (mm2)
4000
3000
2000
1000
0
**
WT
SAG1
GRA4
LiHsp83-SAG1

Fig. 2

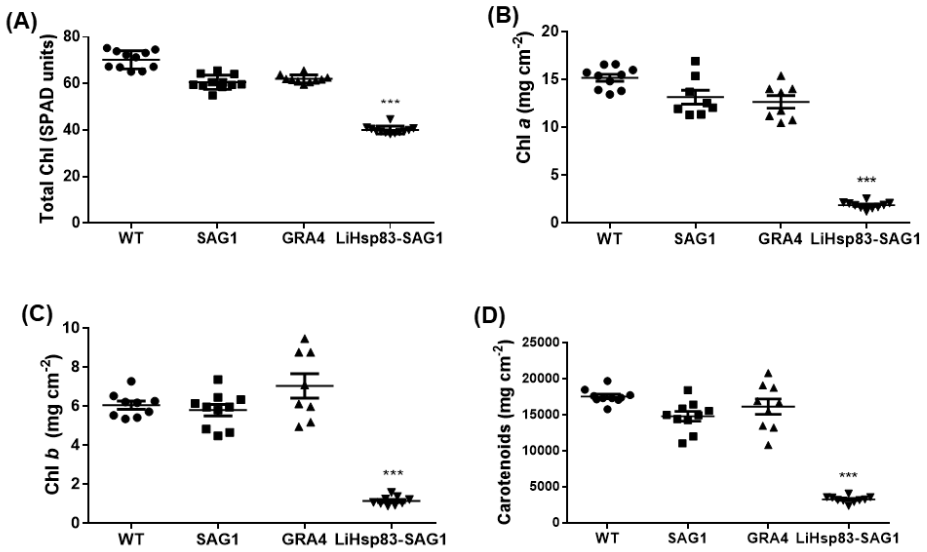
(A)
Total Chl (SPAD units)
0
20
40
60
80
***
WT
SAG1
GRA4
LiHsp83-SAG1
(B)
Chl a (mg cm-2)
0
5
10
15
20
***
WT
SAG1
GRA4
LiHsp83-SAG1
(C)
Chl b (mg cm-2)
0
2
4
6
8
10
***
WT
SAG1
GRA4
LiHsp83-SAG1
(D)
Carotenoids (mg cm-2)
0
5000
10000
15000
20000
25000
***
WT
SAG1
GRA4
LiHsp83-SAG1

Fig. 3

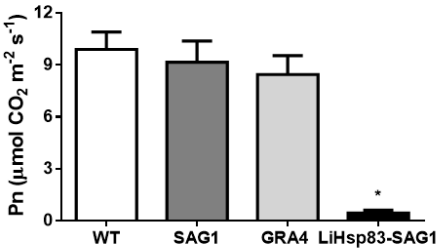

Fig. 4

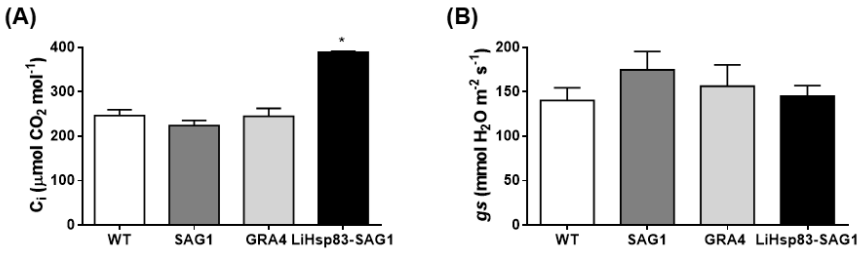
(A)
C_i (µmol CO_2 mol^{-1})
400
300
200
100
0
*
WT
SAG1
GRA4
LiHsp83-SAG1
(B)
gs (mmol H_2O m^{-2} s^{-1})
200
150
100
50
0
WT
SAG1
GRA4
LiHsp83-SAG1

Fig. 5

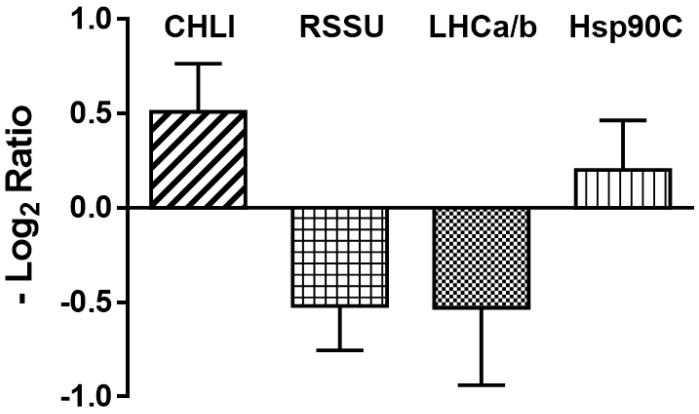

Fig. 6

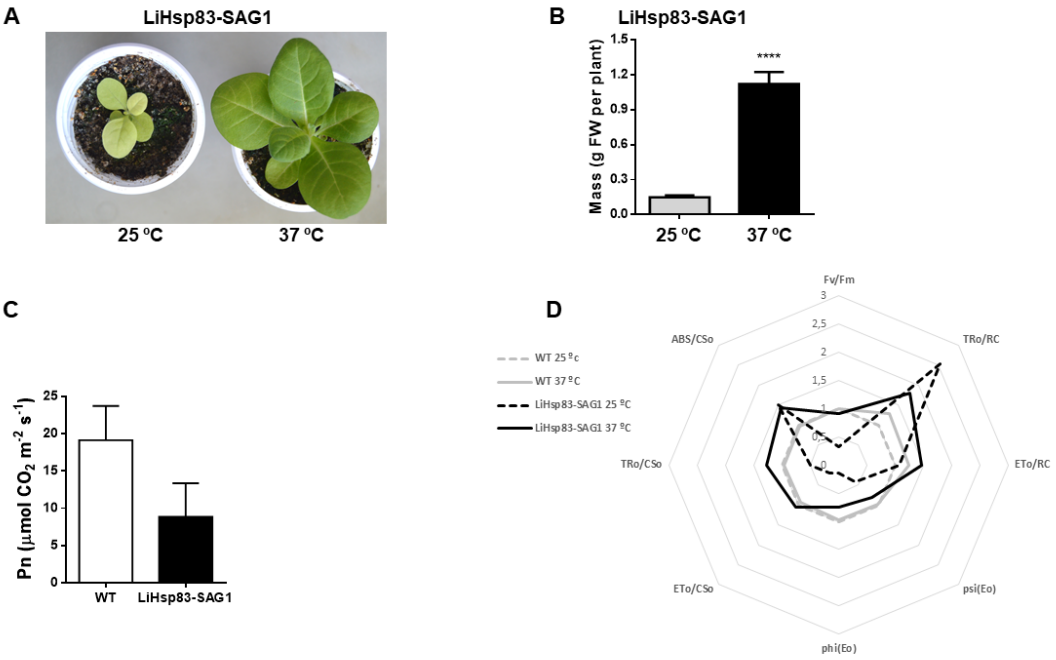
A
LiHsp83-SAG1
25 °C
37 °C
B
LiHsp83-SAG1
Mass (g FW per plant)
1.5
1.2
0.9
0.6
0.3
0.0
****
25 °C
37 °C
C
Pn (μmol CO2 m-2 s-1)
25
20
15
10
5
0
WT
LiHsp83-SAG1
D
WT 25 °c
WT 37 °C
LiHsp83-SAG1 25 °C
LiHsp83-SAG1 37 °C
Fv/Fm
TRo/RC
ETo/RC
psi(Eo)
phi(Eo)
ETo/CSo
TRo/CSo
ABS/CSo
3
2,5
2
1,5
1
0,5
0

Fig. 7

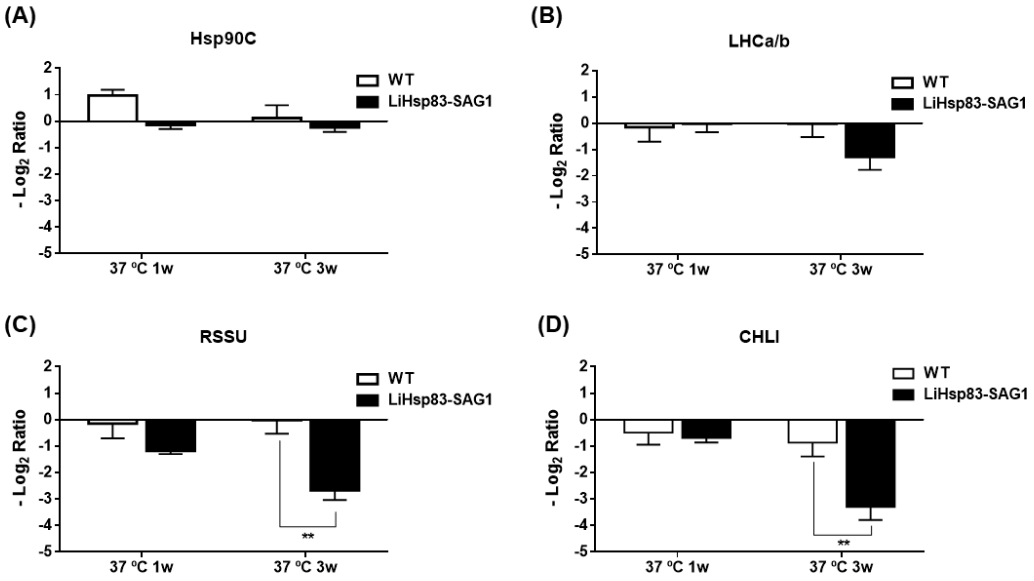
(A)
Hsp90C
WT
LiHsp83-SAG1
- Log2 Ratio
2
1
0
-1
-2
-3
-4
-5
37 ºC 1w
37 ºC 3w
(B)
LHCa/b
WT
LiHsp83-SAG1
- Log2 Ratio
37 ºC 1w
37 ºC 3w
(C)
RSSU
WT
LiHsp83-SAG1
- Log2 Ratio
**
37 ºC 1w
37 ºC 3w
(D)
CHLI
WT
LiHsp83-SAG1
- Log2 Ratio
**
37 ºC 1w
37 ºC 3w

Fig. 8

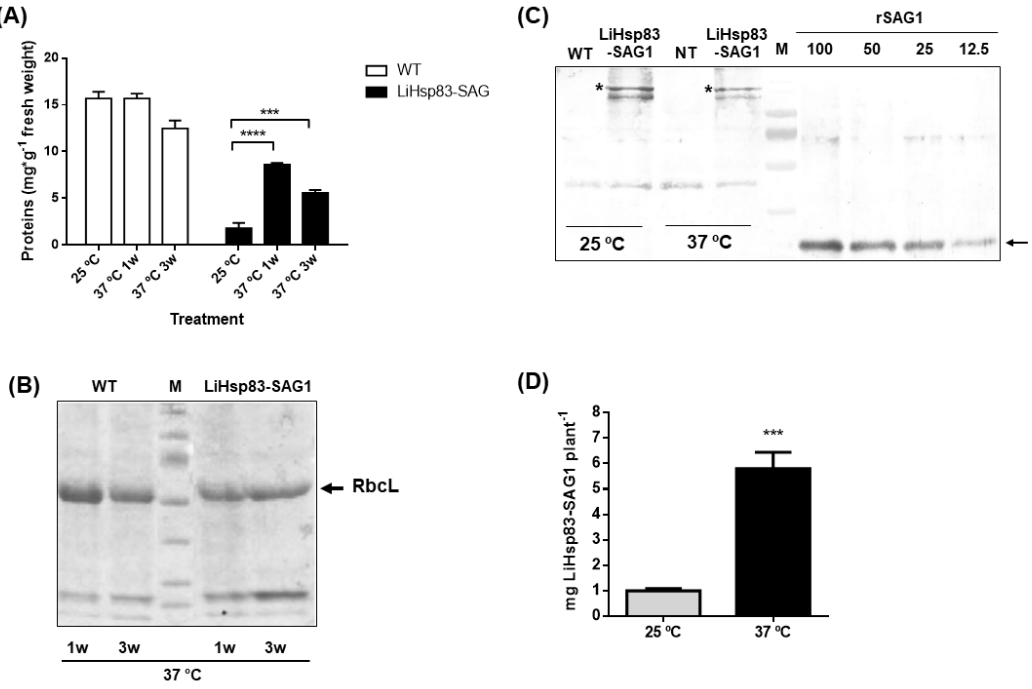
(A)
Proteins (mg g-1 fresh weight)
WT
LiHsp83-SAG
***
****
25 °C
37 °C 1w
37 °C 3w
Treatment
(C)
WT
LiHsp83 -SAG1
NT
LiHsp83 -SAG1
M
rSAG1
100
50
25
12.5
25 °C
37 °C
(B)
WT
M
LiHsp83-SAG1
RbcL
1w
3w
1w
3w
37 °C
(D)
mg LiHsp83-SAG1 plant-1
***
25 °C
37 °C

Table S1

Summary of primer sequences.

PRIMER	SEQUENCE (5' - 3')	REFERENCES
NtEFa-qPCR-867F	TGAGATGCACCACGAAGCTC	Bhor et al., 2017
NtEFa-qPCR-917R	CCAACATTGTCACCAGGAAGTG	Bhor et al., 2017
NtRSSU-qPCR-375F	CGGATTTGTCTACCGTGAAA	Bhor et al., 2017
NtRSSU-qPCR-470R	CATCAGTGCACCCAAACA	Bhor et al., 2017
NtLHCab-qPCR-263F	ACCATCAAACTTGGAGAGATAC	Bhor et al., 2017
NtLHCab-qPCR-373R	GCCCATTCTTGAGCCTTTA	Bhor et al., 2017
NtChlI-qPCR-94F	GCTTCTACACCCTTGTCTTC	Bhor et al., 2017
NtChlI-qPCR-224R	ATTGGGACCTCCCTTTCT	Bhor et al., 2017
Nt-Hsp90C-qPCR-2111F	GGTTGAGCTCATCACCAT	Bhor et al., 2017
Nt-Hsp90C-qPCR-2235R	CTTCTCCCTCTCATAAACTCC	Bhor et al., 2017

Table S2. **List of photosynthetic OJIP parameters**

PARAMETER	DEFINITION
Fv/Fm	maximum quantum yield of primary PSII photochemistry
PI_{ABS}	performance index for energy conservation from photons absorbed by PSII to reduction Q_B
ABS/CSo	absorption flux per cross section
TRo/CSo	trapped flux per cross section
ETo/CSo	electron transport per cross section
ABS/RC	absorption flux per reaction centre
TRo/RC	trapped flux per reaction centre
ETo/RC	electron transport per reaction centre
Phi(Eo)	probability for an electron from Q_B to be transferred to PSI acceptors
Psi(Eo)	probability for a trapped exiton to move an electron into the electron chain beyond Q_A

Supplemental Fig. S1

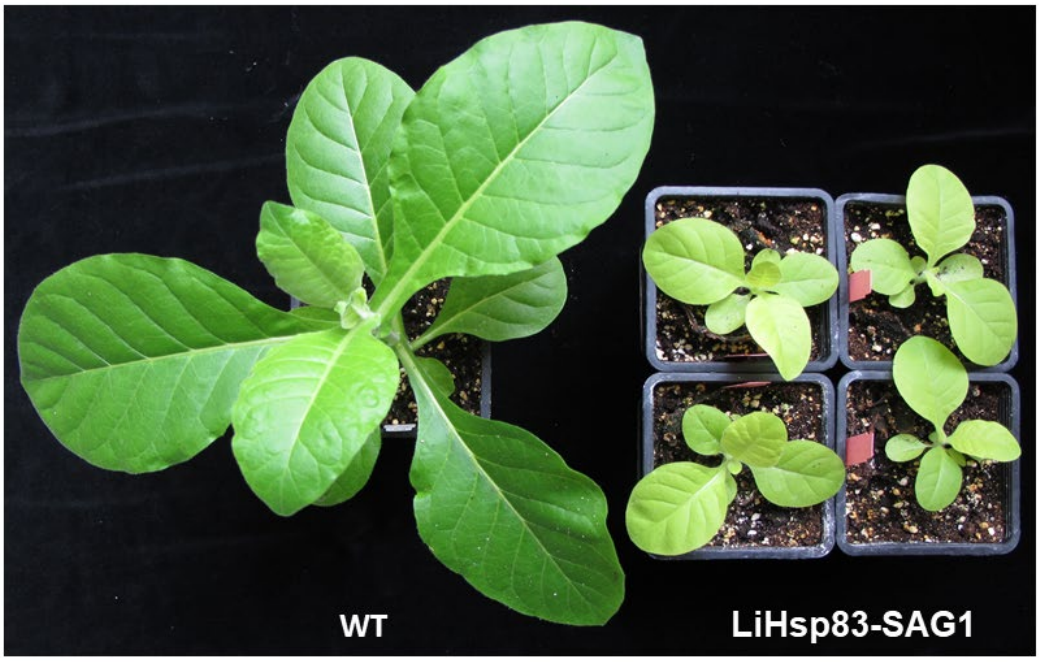

Supplemental Fig. S2

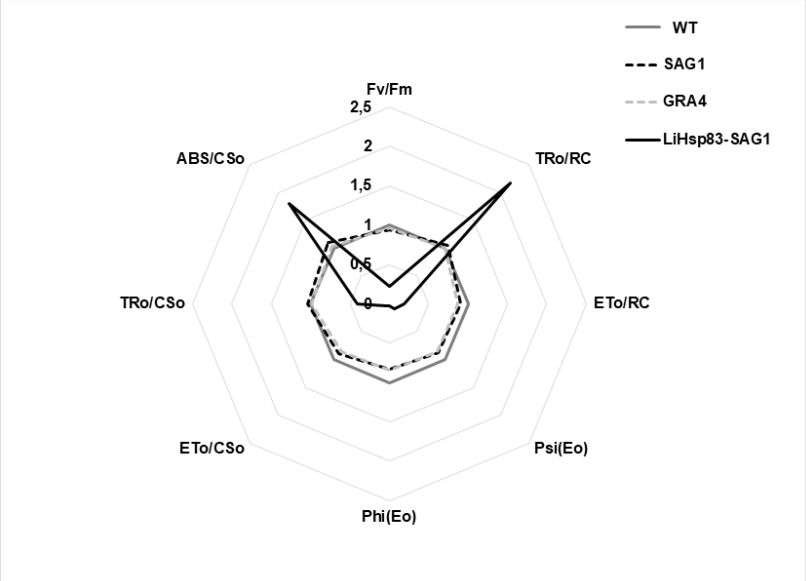

Supplemental Fig. S3

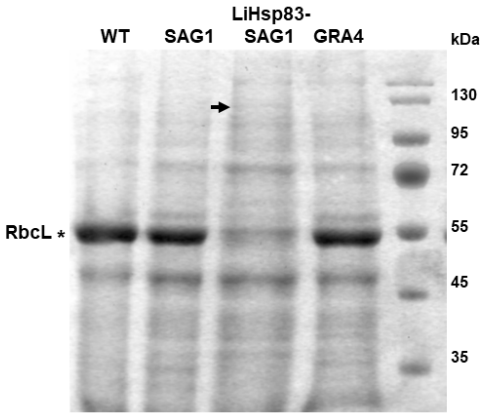

Supplemental Fig. S4